Velocity Control of a Spherical Rolling Robot Using a Grey-PID Type Fuzzy Controller With an Adaptive Step Size

Erkan Kayacan, Erdal Kayacan, Herman Ramon, Wouter Saeys

Division of Mechatronics, Biostatistics and Sensors, Department of Biosystems, KU Leuven, Kasteelpark Arenberg 30, B-3001 Leuven, Belgium. (e-mail: {erkan.kayacan, erdal.kayacan, herman.ramon, wouter.saeys}@biw.kuleuven.be)

Abstract: This paper proposes a grey-PID type fuzzy controller (GPIDFC) with an adaptive step size to control the velocity of a spherical rolling robot characterized by a highly nonlinear system model. The proposed control structure consists of a grey predictor and a PID type fuzzy controller (PIDFC). Another fuzzy controller is proposed to tune the step size of the grey predictor. The simulation results show that the PIDFC coupled to a grey predictor with an adaptive step size is able to control the spherical rolling robot with a better transient response, e.g. lower overshoot, when compared to a conventional PIDFC.

Keywords: spherical rolling robot, fuzzy logic, grey system, adaptive step size, mobile robot

1. INTRODUCTION

A system might be described with a color with respect to the amount of modeling information obtained. For instance, if the mathematical model and/or internal structure of the system are not known, the system can be seen as a *black system*. On the other hand, if the dynamical equations of the system are completely known, the system is considered to be a *white system*. In a similar manner, if the mathematical model and/or internal structure are only partially known, the system is considered to be a *grey system*. In practice, as a system model is always only an abstraction of the real system neglecting some of the uncertainties and perturbations, any real-time system can be considered to be a grey system (Kayacan and Kaynak, 2009, 2006).

Grey predictors aim to predict the future values of a system based-on the current and past values of the system. Each time a new data point is obtained, the oldest value in the original data set is omitted and replaced by the new value. This fact makes grey controllers more robust than the conventional controllers against uncertainties and perturbations on a real-time system. In literature, the most successful implementations of the grey controllers are seen in real time applications.

There are several successful implementations of grey predictors and grey controllers in literature: For example, grey fuzzy controllers have been proposed to handle the uncertainties on the determination of the cutting force of a turning operation, and it is shown experimentally that the grey predictive fuzzy controller can reduce the difficulties in determining an appropriate membership function and fuzzy rules in a conventional fuzzy controller (Lian et al., 2005). Grey predictive control has been proposed for electric furnace, polymerizing-kettle and electro-hydraulic proportional pressure control systems in which the forecasting concept is extended to future and past forecast (Song et al., 2009). The control of an inverted pendulum, a well-known benchmark problem in control engineering, has been demonstrated using grey controllers (Huang and Huang, 2000). Grey control of a ship fin stabilizer is described in (Jiguang et al., 2009). From the simulation results it was concluded that the variable structure robust controller based on grey prediction enhances the performance, while reducing the chattering. Grey predictive controllers were proposed for discrete systems (Zhang and Jiao, 2009). It is demonstrated that it is feasible to use a $GM(0, N)$ model coupled to a PID controller to control a discrete system. In (RongCheng et al., 2008), grey controller design based-on considering the residual error has been analyzed. From the simulation results it was concluded that the controller has better dynamic characteristics and restrains interference more effectively than traditional fuzzy control and standard grey prediction control.

As the combination of a grey predictor with a sliding mode controller has been reported to provide good robustness against uncertainties in the case of an antilock braking system (Kayacan et al., 2009), a similar approach is investigated in this study to control a spherical rolling robot. Motivated by the successful results in (Kayacan et al., 2009), the performance of a grey predictor-based

⋆ This work has been carried out within the framework of the LeCoPro project (grant nr. 80032) of the Institute for the Promotion of Innovation through Science and Technology in Flanders (IWT-Vlaanderen). Wouter Saeys is funded as postdoctoral fellow of the Research Foundation - Flanders (FWO).

PID type fuzzy controller with an adaptive step size for the velocity control of a spherical rolling robot has been investigated in this study.

This paper is organized as follows: The mathematical model of the spherical rolling robot is presented in Section II. Section III introduces the grey system theory. In Section IV, the proposed control structure consisting of a grey predictor and conventional fuzzy PID type controllers is described. Simulation results and comparisons are presented in Section V. Finally, a brief conclusion of the study is given in Section VI.

2. THE MATHEMATICAL MODEL OF A SPHERICAL ROLLING ROBOT

The mathematical model of the spherical rolling robot used in this study is similar to the one presented by (Kayacan et al., 2011). The main difference is that viscous friction has been added to the equations of motion. The most important aspects of the model are repeated in this study, but more details can be found in (Kayacan et al., 2011).

A schematic illustration of the spherical rolling robot is given in Fig. 1.

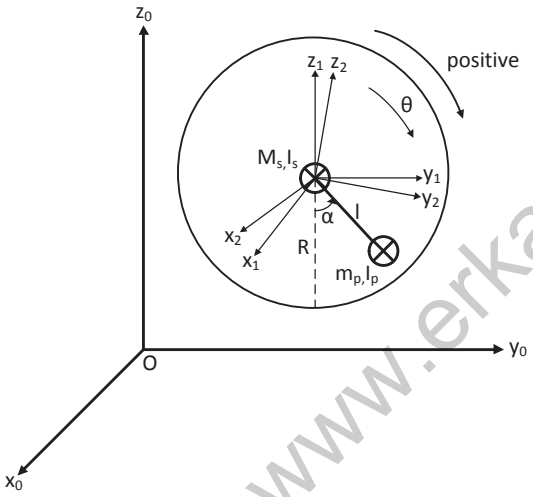

Fig. 1. Modeling of rolling motion about transversal axis for overall translation along $O-y$

2.1 Kinematic Model

The mechanical parameters of the spherical rolling robot are described in Table 1.

The angular velocity vector $\omega_{\mathbf{s}}$ and linear velocity vector $\mathbf{v_s}$ of the center of the sphere, the position vector $\mathbf{r_{p_0}}$, the angular velocity vector $\omega_{\mathbf{p}}$ and the linear velocity vector $\mathbf{v}_p$ of the mass center of the pendulum are given by:

$$\omega_{\mathbf{s}} = -\dot{\theta}\mathbf{i} \tag{1}$$

$$\mathbf{v_s} = -R\dot{\theta}\mathbf{j} \tag{2}$$

$$\mathbf{r_p} = l\sin(\alpha-\theta)\mathbf{j} - l\cos(\alpha-\theta)\mathbf{k} \tag{3}$$

Table 1. NOMENCLATURE

θ	Rolling angle of the sphere around the x axis
α	Degree of freedom of pendulum
M_s	The mass of the sphere
I_s	The mass moment of inertia of the sphere
M_p	The mass of the pendulum
I_p	The inertia moment of the pendulum
R	Radius of the sphere
l	Distance between the center of the sphere and the center of gravity of the pendulum
g	Gravitational acceleration
ζ	Damping coefficient

$$\omega_{\mathbf{p}} = (\dot{\alpha}-\dot{\theta})\mathbf{i} \tag{4}$$

$$\mathbf{v}_p = \big(-R\dot{\theta} + (\dot{\alpha}-\dot{\theta})l\cos(\alpha-\theta)\big)\mathbf{j} + \big((\dot{\alpha}-\dot{\theta})l\sin(\alpha-\theta)\big)\mathbf{k} \tag{5}$$

where θ, α, R and l represent the rolling angle of the sphere around the x axis, the angle of rotation of the pendulum around the x axis, the radius of the sphere and the distance between the center of the sphere and the center of the pendulum, respectively. Similarly, **i**, **j** and **k** represent the unit vector on the x, y and z axes, respectively.

2.2 Dynamic Model

Let E_k and E_p denote respectively the total kinetic and potential energy of the system. With M_s and m_p representing the masses of the sphere and pendulum, I_s and I_p representing the moments of inertia, and v_s, ω_s, v_p and ω_p representing the linear and angular velocities of the sphere and pendulum, r_{p-z} representing the vertical position of the mass center of the pendulum. The Lagrangian function L including only the terms owing to rotations around the transversal axis can then be written as follows:

$$\begin{aligned} L &= E_k - E_p \\ &= \frac{1}{2}M_s\|\mathbf{v_s}\|^2 + \frac{1}{2}I_s\|\omega_{\mathbf{s}}\|^2 + \frac{1}{2}m_p\|\mathbf{v_p}\|^2 + \frac{1}{2}I_p\|\omega_{\mathbf{p}}\|^2 \\ &\quad -m_p g r_{p-z} \\ &= \frac{1}{2}M_s(-R\dot{\theta})^2 + \frac{1}{2}I_s(-\dot{\theta})^2 + \frac{1}{2}I_p(\dot{\alpha}-\dot{\theta})^2 \\ &\quad +\frac{1}{2}m_p\Big(\big(-R\dot{\theta} + (\dot{\alpha}-\dot{\theta})l\cos(\alpha-\theta)\big)^2 \\ &\quad +\big((\dot{\alpha}-\dot{\theta})l\sin(\alpha-\theta)\big)^2\Big) - m_p g l\cos(\alpha-\theta) \end{aligned} \tag{6}$$

It is assumed that the viscous friction operates between the sphere and the surface. The loss due to the viscous friction is written in an energy dissipation function that depends on the velocities of the system and the damping constant:

$$S = \frac{1}{2}\zeta\dot{q}_i^2 = \frac{1}{2}\zeta(\dot{\theta}^2 + \dot{\alpha}^2) \tag{7}$$

For translation along $O-y$, the Euler-Lagrange equations of the system are written as follows:

$$\frac{d}{dt}\Big(\frac{\partial L}{\partial \dot{q}_i}\Big) - \frac{\partial L}{\partial q_i} + \frac{\partial S}{\partial \dot{q}_i} = Q_i \tag{8}$$

where $q_1 = \theta$ and $q_2 = \alpha$ are the generalized coordinates. In fact, when the pendulum is rotated through an input

torque, a reaction torque about the shaft occurs in the opposite direction (Ming et al., 2006).

The input torque to rotate the pendulum is represented by $Q_1 = Q_2 = \tau$.

$$\begin{aligned} Q_\theta &= \tau \\ Q_\alpha &= \tau \end{aligned} \tag{9}$$

The equations of motion of a mechanical system can be written as follows:

$$M\big(q(t)\big)\ddot{q}(t) + C\big(q(t), \dot{q}(t)\big) + G\big(q(t)\big) = u(t) \tag{10}$$

The equations of motion can be finally written in the following matrix form:

$$\begin{bmatrix} M_{11} & M_{12} \\ M_{21} & M_{22} \end{bmatrix} \begin{bmatrix} \ddot{\theta} \\ \ddot{\alpha} \end{bmatrix} + \begin{bmatrix} C_{11} \\ C_{21} \end{bmatrix} + \begin{bmatrix} G_{11} \\ G_{21} \end{bmatrix} = \begin{bmatrix} \tau \\ \tau \end{bmatrix} \tag{11}$$

where

$$\begin{aligned} M_{11} &= M_s R^2 + m_p R^2 + m_p l^2 + I_s + I_p \\ &\quad +2m_p Rl\cos(\alpha - \theta) \\ M_{12} &= M_{21} = -m_p l^2 - I_p - m_p Rl\cos(\alpha - \theta) \\ M_{22} &= m_p l^2 + I_p \\ C_{11} &= m_p Rl\sin(\alpha - \theta)(\dot{\alpha} - \dot{\theta})^2 + \zeta\dot{\theta} \\ C_{21} &= \zeta\dot{\alpha} \\ G_{11} &= -G_{21} = -m_p gl\sin(\alpha - \theta) \end{aligned}$$

3. GREY SYSTEMS THEORY

3.1 GM(1,1) Model

Representation of *GM(m,n)* in grey system theory denotes a model where m is the order of the differential equation and n is the number of the variables. Although there are various grey models, researchers have focused on the *GM(1,1)* model because of its computational simplicity and efficiency.

Since the differential equation (15) of the *GM(1,1)* model has time-varying coefficients, it can adapt itself to any situation. GM(1,1) model is read *Grey model first order one variable*. *GM(1,1)* can only be used when the output values of the system are bigger than zero. Since the velocity of the spherical rolling robot is always bigger than zero due to considering only forward motion of the system, the *GM(1,1)* model can be used for the velocity control of the spherical rolling robot considered in this study. Another critical requirement is that the ratio of the previous data point to the current data point must be in the interval of $[0.1345; 7.389]$ in the grey model $GM(1,1)$ (Deng, 1989).

In the forecasting process, the data set $X^{(0)} = x^{(0)}(1)$, $x^{(0)}(2), x^{(0)}(3)$ and $x^{(0)}(4)$ is used to predict the data point $x^{(0)}(5)$. In the next step, the first data point in $X^{(0)}$ is omitted and the modified data set $X^{(0)} = x^{(0)}(2), x^{(0)}(3), x^{(0)}(4)$ and $x^{(0)}(5)$ are used to predict the data point $x^{(0)}(6)$. This procedure, which can be seen as a time window going through the data set, is repeated during the simulation.

The data set consisting of the output values of a system is denoted as $X^{(0)}$:

$$X^{(0)} = \Big(x^{(0)}(1), x^{(0)}(2), ..., x^{(0)}(n)\Big), n \geq 4 \tag{12}$$

Accumulating generation operation (AGO) is defined in (13), and the sequence $X^{(1)}$ is obtained,

$$X^{(1)} = \Big(x^{(1)}(1), x^{(1)}(2), ..., x^{(1)}(n)\Big), n \geq 4 \tag{13}$$

where

$$x^{(1)}(k) = \sum_{i=1}^{k} x^{(0)}(i), k = 1, 2, 3....., n \tag{14}$$

The tendency of the generated sequence $X^{(1)}$ can be approximated by using an exponential function. As the behavior of a first order differential equation is similar to an exponential function, the first order ordinary differential grey model GM(1,1) can be established as:

$$\frac{dX^1(t)}{dt} + aX^{(1)}(t) = b \tag{15}$$

where the parameters a and b represent the development coefficient and grey action quantity, respectively. These parameters can be found through least squares estimation:

$$\begin{bmatrix} a \\ b \end{bmatrix} = (B^T B)^{-1} B^T Y \tag{16}$$

where

$$Y = \Big[x^{(0)}(2), x^{(0)}(3), ..., x^{(0)}(n)\Big]^T \tag{17}$$

$$B = \begin{bmatrix} -\frac{1}{2}[x^{(1)}(2) + x^{(1)}(1)] & 1 \\ -\frac{1}{2}[x^{(1)}(3) + x^{(1)}(2)] & 1 \\ . & . \\ . & . \\ . & . \\ -\frac{1}{2}[x^{(1)}(n) + x^{(1)}(n-1)] & 1 \end{bmatrix} \tag{18}$$

By solving (15), $x^{(1)}(k)$ is obtained as:

$$\hat{x}^{(1)}(k) = \left[\hat{x}^{(0)}(1) - \frac{b}{a}\right] e^{-ak} + \frac{b}{a} \tag{19}$$

After the process of AGO, the inverse accumulated generating operation (IAGO), which is defined in (20), has to be applied to obtain the original data set. The operation of IAGO for the first order series is defined as follows:

$$\begin{aligned} x^{(0)}(1) &= x^{(1)}(1) \\ x^{(0)}(k) &= x^{(1)}(k) - x^{(1)}(k-1), k = 2, 3, ..., n. \end{aligned} \tag{20}$$

Another way of obtaining $\hat{x}^{(0)}(k)$ is as follows:

$$\hat{x}^{(0)}(k) = \left[\hat{x}^{(0)}(1) - \frac{b}{a}\right] e^{-ak}(1 - e^a) \tag{21}$$

The predicted value of the data set at step H is written as follows:

$$\hat{x}^{(0)}(k+H) = \left[\hat{x}^{(0)}(1) - \frac{b}{a}\right] e^{-a(k+H+1)}(1 - e^a) \tag{22}$$

4. THE CONTROL SCHEME

4.1 PID Type Fuzzy Controller

The rule base used in the PD type fuzzy controller is shown in Table 2. The first column and row contain linguistic representations of the error e and time derivative of the error de/dt, respectively. The membership functions of the inputs and the output are chosen as triangular membership functions which are equally distributed over the support. The supports of the membership functions for the input 1 and input 2 are $[-0.05; 0.25]$ and $[-1.5; 0.3]$, respectively. Similarly, the support of the membership functions for the output is $[-4; 4]$. The number of membership functions for each variable is chosen as equal to 7 resulting in 49 rules. NL, NM, NS, ZR, PS, PM and PL stand for negative large, negative medium, negative small, zero, positive small, positive medium and positive large, respectively.

Table 2. Rule Base for a PD type Fuzzy Controller

$\Delta e/e$	**NL**	**NM**	**NS**	**ZR**	**PS**	**PM**	**PL**
PL	ZR	PS	PM	PL	PL	PL	PL
PM	NS	ZR	PS	PM	PL	PL	PL
PS	NM	NS	ZR	PS	PM	PL	PL
ZR	NL	NM	NS	ZR	PS	PM	PL
NS	NL	NL	NM	NS	ZR	PS	PM
NM	NL	NL	NL	NM	NS	ZR	PS
NL	NL	NL	NL	NL	NM	NS	ZR

As can bee seen from Table 2, there are $7 \times 7 = 49$ rules for the PD type fuzzy controller. If a PID type fuzzy controller is desired to take both advantages of PD and PI type fuzzy controllers, integral action is added to the PD type fuzzy controller. Thus, the number of total rules will be $7 \times 7 \times 7 = 343$. In practice, this requires more computational effort and also results in much time to tune the controller. To avoid the drawbacks mentioned above, as shown in Fig. 2, the output of the PD type fuzzy controller is multiplied by β and α which are the weights of PI and PD type fuzzy controllers. Therefore, in that case, PI and PD type fuzzy controllers are working in a parallel structure. The bigger the α/β ratio, the more important the derivative effect will become.

4.2 Grey predictor

In the grey predictive control approach, the outputs of the grey predictor are used instead of the current outputs of the system. The block diagram of the proposed grey predictive controller with an adaptive step size is shown in Fig. 2. The block diagram in Fig. 2 also shows that a second fuzzy controller, i.e. the step size controller, is included for the determination of the step size of the grey predictor. The inputs of the step size controller are the error and the time derivative of the error. The membership functions of the inputs and the output are chosen as triangular membership functions which are equally distributed over the support. The supports of the membership functions for input 1 and input 2 are the same with the ones in Table 2. Similarly, the support of the membership functions for the output is $[15; 30]$. The related rule base is shown in Table 3. VL, L, RL, M, RS, S and VS stand for very long, long, rather long, medium, rather short, short and very short, respectively. It is to be noted that $V\big(q(t), \dot{q}(t)\big) = C\big(q(t), \dot{q}(t)\big) + G\big(q(t)\big)$ in Fig. 2.

Table 3. A general Rule Base for a Step Size Controller

$\Delta e/e$	**PL**	**PM**	**PS**	**ZR**	**NS**	**NM**	**NL**
PL	L	RL	RS	VS	VS	S	S
PM	RL	M	RS	RS	S	RS	RS
PS	M	S	VS	RL	L	RL	M
ZR	M	RL	L	VL	L	RL	M
NS	M	LS	S	RL	VS	S	RS
NM	RS	S	S	M	S	M	RL
NL	S	VS	VS	VS	S	RL	L

4.3 Feedback Linearization

Feedback linearization is a closed-loop control design for nonlinear systems. The main idea in feedback linearization is to algebraically transform the nonlinear dynamics into linear dynamics through appropriate feedback, such that the resulting closed-loop linear dynamics can be easily governed by linear control techniques. Feedback linearization is frequently used in control of serial manipulators and known as *computed torque control* in robotics literature (Craig, 2005). By using feedback linearization method, the nonlinearities presented will be compensated in a closed-loop fashion.

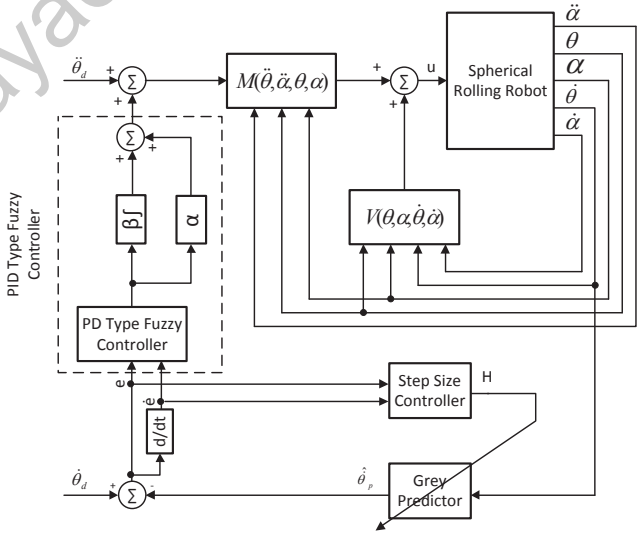

Fig. 2. Block diagram of the adaptive grey fuzzy PID controller structure for feedback linearization

5. SIMULATION RESULTS AND DISCUSSION

The numerical values used in this study are $M_s = 3\ kg$, $m_p = 2\ kg$, $R = 0.2\ m$, $l = 0.075\ m$ and $g = 9.81\ m/s^2$. The damping coefficient, ζ, in the equations of motion is set to 0.3 for Fig. 3-5, and the sampling period of the simulations is set to $0.01\ s$. The input torque u is limited by a saturation for a maximum value of $2.5\ Nm$ for all the simulations.

The controller gains are selected such that the required input torque does not exceed the maximum value allowed

by the actuators, i.e. 2.5 Nm. The coefficients of the PIDFCs were tuned to $\alpha = 0.2$ and $\beta = 0.2$ by trial-and-error method.

In Fig. 3, the step responses of the PIDFC controller and the combination of the grey predictor with this PIDFC controller are presented. The GPIDFC results in a smaller rise time, overshoot and settling time. It can be concluded that the control scheme with the proposed GPIDFC is able to improve the transient response performance of the system.

In Fig. 4, the step responses of the GPIDFCs with a fixed step size and a variable step size are compared. GPIDFCs with a variable step size results in smaller rise time and smaller overshoot.

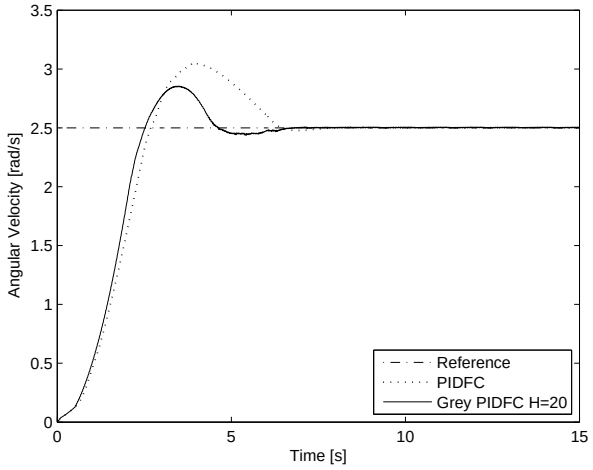

Fig. 3. The velocity response of the system for PIDFC and GPIDFC with a fixed step size

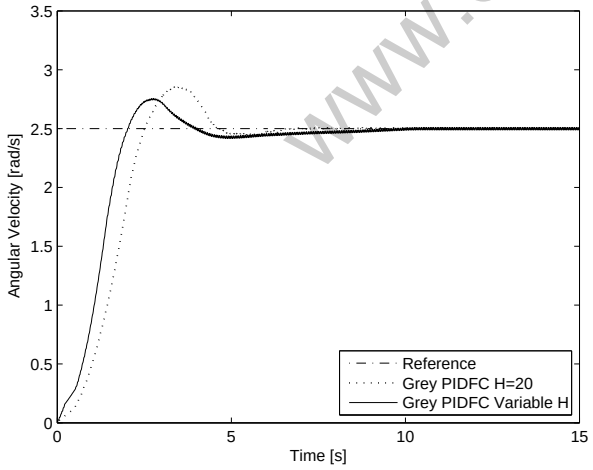

Fig. 4. The velocity response of the system for GPIDFCs with a fixed step size and a variable step size

As a next step, the output of the system is again simulated as if it was measured with a noise level $SNR = 40dB$ and the following reference signal has been applied to the system (23):

$$\text{Reference}(t) = \begin{cases} 2.5 \text{ rad/s} & \text{if } 0 < t \leq 10 \\ 3 \text{ rad/s} & \text{if } 10 < t \leq 20 \\ 2 \text{ rad/s} & \text{if } 20 < t \leq 30 \end{cases} \quad (23)$$

To test the robustness of this variable step size approach, noise is added to the output signal to simulate the effect of a feedback sensor with an SNR of $40dB$. In Fig. 5, the responses of the GPIDFCs with a fixed step size and a variable step size are illustrated. It can be observed that the GPIDFC with a variable step size is more robust to the uncertainties and gives more satisfactory results regarding smaller overshoot than the GPIDFC with a fixed step size. Figure 6 shows the zoomed view of Fig. 5 between $0^{th} - 9^{th}$ seconds.

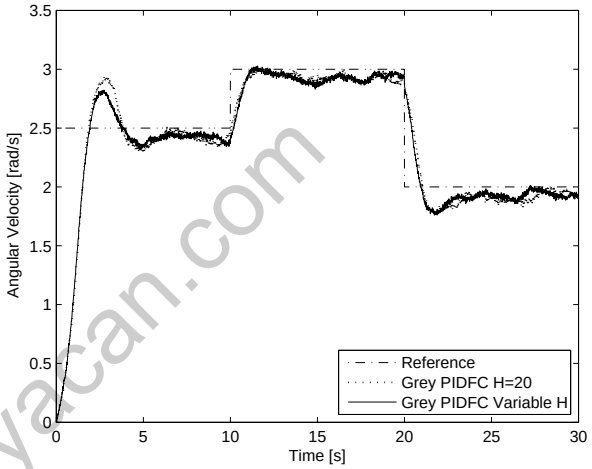

Fig. 5. The velocity response of the system for GPIDFCs with a fixed step size and a variable step size when the reference is set to 2.5 rad/s, 3 rad/s and 2 rad/s at 0^{th} second, 10^{th} second and 20^{th} second, respectively

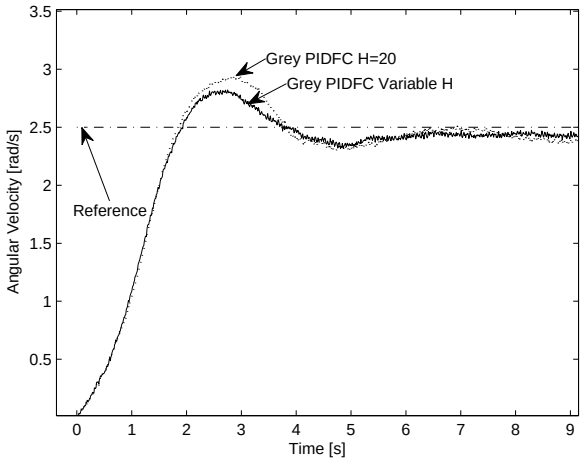

Fig. 6. The zoomed view of Fig. 5 between $0^{th} - 9^{th}$ seconds.

As the last step in the simulation studies, the following variation of the damping coefficient over time was applied to the system to test the robustness of the controllers:

$$\zeta(t) = \begin{cases} 0.3 & \text{if } 0 < t \leq 10 \\ 0.5 & \text{if } 10 < t \leq 20 \\ 0.3 & \text{if } 20 < t \leq 30 \end{cases} \quad (24)$$

The velocity responses of the GPIDFCs with a fixed step size and a variable step size are shown in Fig. 7. As can be seen from that figure, the GPIDFC with a variable step size can adapt its parameters when the coefficient of viscous friction changes suddenly. For the case when the coefficient of the viscous friction changes, the response of the system controlled by the GPIDFC with variable step has less overshoot than the response of the system controlled by the GPIDFC with fixed step. From these simulations it can be concluded that both controllers are robust thanks to the grey system approach.

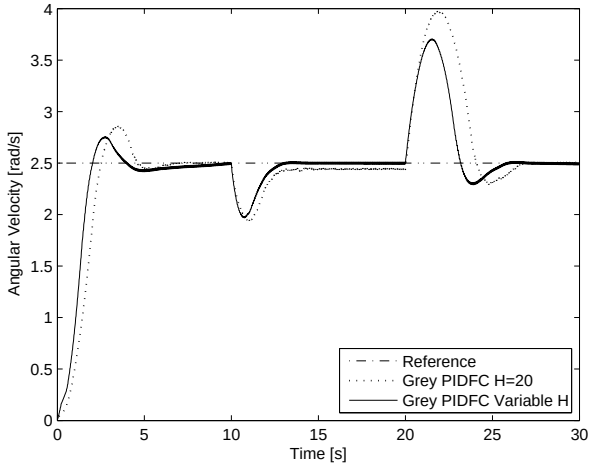

Fig. 7. The velocity response of the system for GPIDFCs with a fixed step size and a variable step size when the damping coefficient is set to 0.3, 0.5 and 0.3 at 0^{th} second, 10^{th} second and 20^{th} second, respectively

When the results in this paper are compared to the previous study in which a conventional PD type fuzzy controller is used (Kayacan et al., 2011), it can be concluded that the GPIDFC with an adaptive step size has better control capability of the spherical rolling robot. The qualitative comparison of grey predictors with a fixed step size and an adaptive step size are given in Table 4.

Table 4. Mean Squared Error

Cases	Method	
	GPIDFC with a fixed step size	GPIDFC with a variable step size
Step response	0.4561	0.3079
Different step responses when the output of the system is measured with a noise level $SNR = 40dB$	0.1739	0.1723
Step responses when the output of the system is measured with a noise level $SNR = 40dB$	0.3128	0.3011
Different damping coefficients	0.3988	0.2534

6. CONCLUSION

In this study, a grey PID type fuzzy controller with an adaptive step size has been proposed for the control of a spherical rolling robot. The system has been controlled with a combination of feedback linearization, a PID type fuzzy controller and a grey predictor simultaneously. The performance of the proposed control scheme has been evaluated in simulation and compared to the performance of a PID controller and a PID type fuzzy controller. The proposed adaptive grey PID type fuzzy controller outperforms the other controllers in terms of overshoot and settling time.

REFERENCES

Craig, J.J. (2005). *Introduction to Robotics: Mechanics and Control*. Prentice Hall.

Deng, J.L. (1989). Introduction to grey system theory. *The Journal of Grey System*, 1, 1 – 24.

Huang, S.J. and Huang, C.L. (2000). Control of an inverted pendulum using grey prediction model. *IEEE Trans. on Industrial Application*, 36, 452–458.

Jiguang, S., HongZhang, J., Lihua, L., and Hongyu, S. (2009). Variable structure control based on grey prediction for ship fin stabilizer. In *Proceedings of IEEE International Symposium on Industrial Electronics*, 620–625. Korea.

Kayacan, E., Bayraktaroglu, Z.Y., and Saeys, W. (2011). Modeling and control of a spherical rolling robot: A decoupled dynamics approach. *Robotica*. doi: 10.1017/S0263574711000956.

Kayacan, E. and Kaynak, O. (2006). Grey prediction based control of a non-linear liquid level system using pid type fuzzy controller. In *IEEE International Conference on Mechatronics*, 292 –296. doi: 10.1109/ICMECH.2006.252541.

Kayacan, E. and Kaynak, O. (2009). An adaptive grey PID-type fuzzy controller design for a non-linear liquid level system. *Transactions of the Institute of Measurement and Control*, 31, 33–49.

Kayacan, E., Oniz, Y., and Kaynak, O. (2009). A grey system modeling approach for sliding-mode control of antilock braking system. *IEEE Transactions on Industrial Electronics*, 56(8), 3244–3252.

Lian, R.J., Lin, B.F., and Huang, J.H. (2005). A grey prediction fuzzy controller for constant cutting force in turning. *International Journal of Machine Tools and Manufacture*, 45, 1047–1056.

Ming, Y., Zongquan, D., Xinyi, Y., and Weizhen, Y. (2006). Introducing hit spherical robot: Dynamic modeling and analysis based on decoupled subsystem. In *Proceedings of the IEEE International Conference on Robotics and Biomimetics*, 181–186. Harbin, China.

RongCheng, L., WenZhan, D., and Sen, X. (2008). A adaptive grey fuzzy prediction controller design based on the improving residual error model. In *Proceedings of IEEE Conference on Cybernetics and Intelligent Systems*, 652 – 656. China.

Song, W., Xiao, J., and Wang, G. (2009). Switching grey prediction fuzzy control for electro-hydraulic proportional pressure control system. In *Proceedings of of the 2009 IEEE International Conference on Mechatronics and Automation*, 850 – 854. China.

Zhang, Y. and Jiao, Z. (2009). Study of grey PID control for discrete system. In *Proceedings of International Workshop on Intelligent Systems and Applications*, 1–4. China.